Solutions of Unsteady-State Radial Gas Flow

R. D. CARTER
JUNIOR MEMBER AIME

PAN AMERICAN PETROLEUM CORP.
TULSA, OKLA.

ABSTRACT

Numerical solutions are presented to some problems of unsteady-state radial flow of gas in which Darcy's law holds. These solutions are intended to aid in explaining the observed behavior of gas wells during drawdown tests. The variation of viscosity and Z-factor with pressure is accounted for in the solutions.

Results are presented for three types of problems: (1) unfractured wells producing at a constant rate, (2) fractured wells producing at a constant rate and (3) unfractured wells producing through a critical flow prover. In the critical-flow-prover solutions, a correction of the calculated well-bore pressure to account for non-Darcy flow is made.

A good correlation is shown between the solutions to the problem of Type 1 and the corresponding diffusivity-equation solution. Using this correlation, the diffusivity solution may be used to obtain gas-well solutions. The solutions to the problems of Type 2 illustrate the difference in drawdown-curve behavior to be expected between fractured and unfractured gas wells. Methods for estimating fracture radius and flow capacity are presented and verified from solutions of Type 2. The solutions to the problems of Type 3 illustrate the differences to be expected between critical-flow-prover drawdown tests and constant-rate tests. An equation is presented for correcting critical-flow-prover data to constant-rate conditions.

A description of the methods used in obtaining the solutions appears in the Appendix.

INTRODUCTION

It is necessary for many engineering purposes, such as predicting future deliverability performance, to be able to relate bottom-hole flowing pressure, formation pressure and flow rate for conditions of stabilized flow in gas wells. This information is customarily given as a plot of $(p_i^2 - p_{wf}^2)$ vs q_g on logarithmic co-ordinates.

It is desirable to be able to predict stabilized performance curves for gas wells based on data obtained from drawdown tests of short duration. Tests of long duration may be wasteful of gas, and low-permeability wells do not stabilize in a short-duration test.

Although it is now commonly recognized that non-Darcy flow plays a significant part in gas-well behavior, it is believed that an understanding of transient behavior of systems obeying Darcy's law is still important in the interpretation of short-term test data, and the prediction of stabilized performance curves therefrom.

In this connection, an equation for correcting Darcy flow solutions for non-Darcy flow effects has existed in the literature for some time. This equation is

$$(p_L^2 - p_{wf}^2) = B_1 q_g^2 \quad \ldots\ldots\ldots \quad (1)$$

It seems likely that solutions of the type presented herein, combined with the non-Darcy flow correction of the type of Eq. 1 and the usual laminar-flow skin factor, could provide a model which would adequately explain transient gas-well behavior for times after the non-Darcy flow region (which should be confined to a small area surrounding the well) has been established.

The solutions presented in this paper are for three types of problems: (1) unfractured wells producing at a constant rate, (2) fractured wells producing at a constant rate and (3) unfractured wells producing through a critical flow prover. In the problems of Types 1 and 2, no corrections for non-Darcy flow were made in the results presented, since it was reasoned that the constant-rate boundary condition would facilitate such a correction if it was desired later. For the problems of Type 3, however, a condition of varying flow rate required that a non-Darcy flow correction of the type of Eq. 1 be included. This was done.

Based on the numerical results presented, a number of approximations and a correlation are presented which may be useful in analyzing gas-well test data.

TYPE 1 PROBLEMS—UNFRACTURED WELL, CONSTANT FLOW RATE

It is assumed that the system can be described as a finite cylindrical gas reservoir produced by a single cylindrical well located at the center of the reservoir. Flow is strictly radial.

When the flow obeys Darcy's law, the governing differential equation is[1]

$$\frac{\partial}{\partial R}\left[M(p)\frac{\partial p}{\partial R}\right] = f(R)\,\frac{\partial}{\partial t}\left(\frac{p}{Z}\right) \quad \ldots\ldots \quad (2)$$

where $M(p) = (2.703 \times 10^{-6} \times 520)\left(\frac{khp}{T\mu Z}\right)$, and

$$f(R) = \left(\frac{2\pi \times 520 \times 24}{14.7}\right)\left(\frac{\phi h e^{2R}}{T}\right).$$

Boundary and initial conditions are:

$$M(p)\frac{\partial p}{\partial R} = q_g, \qquad R = R_w;$$

$$\frac{\partial p}{\partial R} = 0, \qquad R = R_e;$$

$$p(R, 0) = p_i \quad \ldots\ldots\ldots\ldots \quad (3)$$

Tables 1 and 2 contain the three sets of problem conditions for which solutions were obtained to the problem

Original manuscript received in Society of Petroleum Engineers office Aug. 7, 1961. Revised manuscript received Feb. 27, 1962. Paper presented at 36th Annual Fall Meeting, Oct. 8-11, 1962, in Dallas.

[1]References given at end of paper.

TABLE 1—PROBLEM CONDITIONS FOR SOLUTIONS 1 AND 2

Reservoir and Well Properties

r_w	0.5 ft
r_e	2,980 ft
ϕ	15 per cent
h	25 ft
T	615° R
k_g	2 md
p_i	3,300 psia

Gas Properties

Pressure (psia)	μ_g (cp)	Z
500	.01249	0.958
1000	.01328	0.924
1500	.01460	0.896
2000	.01605	0.879
2500	.01794	0.870
3000	.01961	0.880
3500	.02127	0.904

Flow Rates

Solution 1: q_g = 2,800 Mcf/D
Solution 2: q_g = 4,000 Mcf/D

TABLE 2—PROBLEM CONDITIONS FOR SOLUTION 3

Reservoir and Well Properties

r_w	0.5 ft
r_e	2,980 ft
ϕ	1.5 per cent
h	12 ft
T	685° R
k_g	0.67 md
p_i	4,700 psia

Gas Properties

Pressure (psia)	μ_g (cp)	Z
500	0.01500	0.965
1000	0.01615	0.933
1500	0.01740	0.910
2000	0.01870	0.895
2500	0.02000	0.890
3000	0.02140	0.901
3500	0.02280	0.922
4000	0.02420	0.950
4500	0.02560	0.983
5000	0.02710	1.015

Flow Rate

Solution 3: q_g = 1,200 Mcf/D

defined by Eqs. 2 and 3. Figs. 1 and 2 show the early portion of the solutions for these conditions which is unaffected by the external boundary. The solutions are plotted as $(p_i^2 - p_L^2)$ vs time on a logarithmic scale. The method of the solution is treated in the Appendix.

DIFFUSIVITY-EQUATION CORRELATION

There should be some similarity between the results shown in Figs. 1 and 2 which are unaffected by the external boundary and the solution to the diffusivity-equation problem for the region bounded internally by a cylinder and with boundary and initial conditions corresponding to Eq. 3 (except that the external radius is infinite).[2]

Fig. 3 is a comparison of Solutions 1, 2 and 3 and the diffusivity-equation solution. The gas-equation solutions were made dimensionless by means of the following equations.[3]

$$p_D(t_D) = \frac{p_i^2 - p_L^2(t)}{\left(\frac{1424\,\overline{\mu}\overline{Z}T\,q_g}{k_g h}\right)} \quad \ldots\ldots\ldots \quad (4)$$

$$t_D = \frac{2.634 \times 10^{-4}\, k_g \overline{p} t}{\overline{\mu}\,\phi\, r_w^2} \quad \ldots\ldots\ldots \quad (5)$$

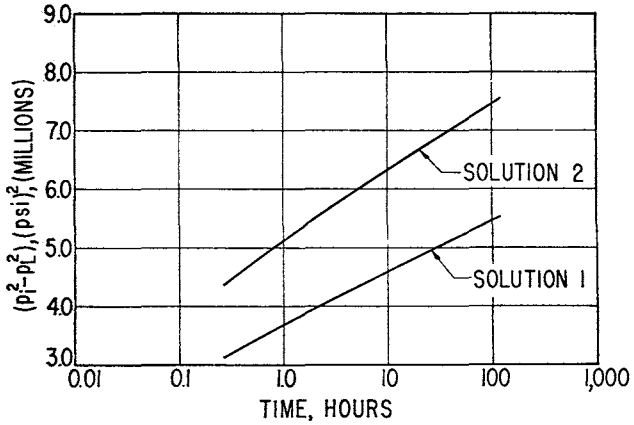

FIG. 1—DRAWDOWN CURVES FROM SOLUTIONS 1 AND 2.

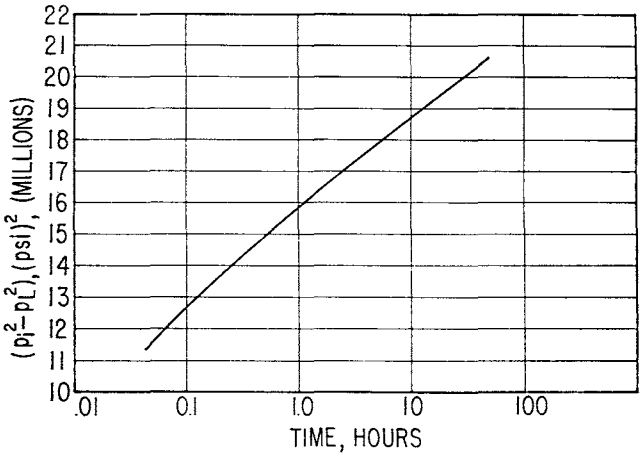

FIG. 2—DRAWDOWN CURVE FROM SOLUTION 3.

where $\overline{\mu} = \mu(\overline{p})$, $\overline{Z} = Z(\overline{p})$, and $\overline{p} = \left(\frac{p_i^2 + p_L^2(t)}{2}\right)^{\frac{1}{2}}$.

In converting the gas-equation solutions to dimensionless form, the quantities $\overline{p}$, $\overline{\mu}$ and $\overline{Z}$ are evaluated anew for each value of p_L. Thus, values of $(p_i^2 - p_L^2)$ and time are not multiplied by constants to obtain the correlation shown in Fig. 3. In the time range shown in Fig. 3, $p_D(t_D) = \frac{1}{2}(\ln t_D + .809)$ is the equation which closely approximates the diffusivity curve. As a comparison, a curve is included in Fig. 3 for Solution 3 in which $[p_i^2 - p_L^2(t)]$ and t are multiplied by constants to convert to dimensionless quantities. This curve diverges noticeably from the diffusivity-equation-solution curve, while the others obtained using the correlation just described remain in good agreement throughout the range presented. Using this correlation, transient gas-well behavior may be estimated from the diffusivity solution presented. It should be emphasized that this correlation is based on instantaneous values of $\overline{p}$, $\overline{\mu}$ and $\overline{Z}$, and not on constant values of these quantities.

These results indicate that a correlation of this type can be obtained when the viscosity and Z-factor functions of pressure are similar in shape to those given in Tables 1 and 2. It seems possible that a more general correlation might be obtained if $\overline{\mu Z}$ were defined by a relation involving an integral, such as $\frac{p_i^2 - p_L^2}{2\int_{p_L}^{p_i} \frac{p}{\mu Z} dp}$, since such a correlation

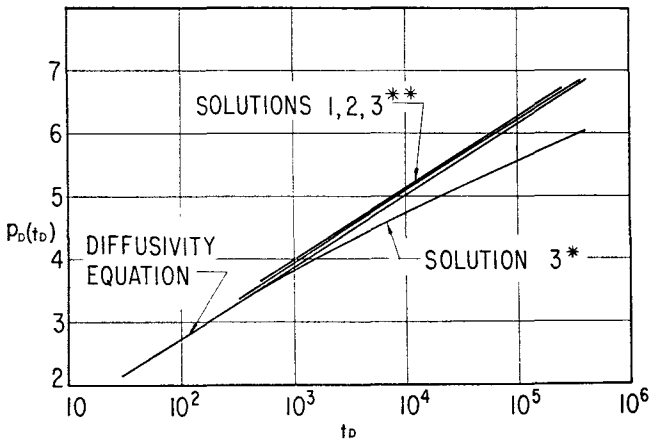

FIG. 3—CORRELATION OF GAS-EQUATION SOLUTIONS AND DIFFUSIVITY-EQUATION SOLUTION. *CONVERTED TO DIMENSINOLESS FORM USING CONSTANT VALUES OF $\bar{p}$, $\bar{\mu}$ AND $\bar{Z}$; **CORRELATED ON THE BASIS OF INSTANTANEOUS VALUES OF $\bar{p}$, $\bar{\mu}$ AND $\bar{Z}$.

would take into account shape variations of the curve of μZ vs p.

STABILIZED FLOW

Stabilized flow is defined here as flow occurring after the pressure disturbance caused by producing the well has reached the external boundary.

A comparison was made between values of $(p_i^2 - p_L^2)$ obtained using a relation in the literature and as obtained from Solution 2.

An equation has been given by Janicek and Katz[9] relating $(p_i^2 - p_L^2)$ to q_g for stablized flow. This equation is

$$(p_i^2 - p_L^2) = \frac{1424\,\overline{\mu Z}\,T\,q_g}{k_g h} \ln \frac{.606\,r_e}{r_w} \quad . \quad . \quad . \quad (6)$$

In Solution 2, at 384 days, a time long enough for stabilization to have been completed, $(p_i^2 - p_L^2)$ was found to be 8.57×10^6 (psi)^2. From Eq. 6, $(p_i^2 - p_L^2)$ was calculated to be 8.62×10^6 (psi)^2. In using Eq. 6, $\bar{p}$ was taken to be $\sqrt{\frac{1}{2}(p_i^2 + p_L^2)}$. This indicates that the approximation of Eq. 6 is acceptable.

MEASUREMENT OF FLOW CAPACITY FROM DRAWDOWN CURVES

Table 3 shows values of permeability-thickness product as employed to obtain Solutions 1, 2 and 3, and as calculated using the equation

$$k_g h = \frac{1637\,q_g \overline{\mu Z} T}{m} \quad . \quad . \quad . \quad . \quad . \quad . \quad . \quad . \quad . \quad . \quad (7)$$

where m is the instantaneous slope, in psi^2 per cycle, read graphically from Figs. 1 and 2 at $t = 10$ hours. Eq. 7 was developed by Tracy.[4] Eq. 7 is equivalent to an equation found in Ref. 3 but, perhaps, is in a more convenient form. Good agreement is shown in Table 3 between actual values of $k_g h$ and those obtained using Eq. 7. It is apparent from the correlation shown in the previous section that better agreement would have been obtained if an appropriate equation similar to Eq. 7 had been used with the slope obtained from a plot of $\frac{(p_i^2 - p_L^2)}{\overline{\mu Z}}$ vs $\ln \frac{\bar{p}t}{\bar{\mu}}$.

TABLE 3—COMPARISON OF kh VALUES USED IN SOLUTIONS 1, 2 AND 3, AND kh VALUES CALCULATED USING EQ. 7

Solution	kh	kh from Eq. 7
1	50	53
2	50	55.3
3	8	10.92

TYPE 2 PROBLEMS—FRACTURED WELLS, CONSTANT FLOW RATE

It is assumed that the fractured well system can be regarded as two zones of different permeability in concentric series, as shown in Fig. 4. This model for a fractured well system is believed to be realistic when the pay has been penetrated by a horizontal, approximately circular fracture and the quantity [(h/r_f) (permeability in the horizontal direction)/(permeability in the vertical direction)$^{\frac{1}{2}}$] is small. Eqs. 2 and 3, together with the additional boundary conditions of Fig. 4, constitute the problem solved. Table 4 shows the problem conditions for Solutions 4 and 5.

FLOW CAPACITY OF FRACTURED AND INTERWELL ZONES

Calculations were made from results from Solutions 4 and 5 to determine the applicability of Eq. 7 to fractured wells. Fig. 5 shows the results $(p_i^2 - p_L^2)$ as a function of time for the conditions given in Table 4. Also shown in Fig. 5 are the values for permeability-thickness product calculated from the straight-line portions of the curves using Eq. 7. The early, flat portions of the curves are due to the fracture; the later, steeper, straight-line portions of the curve reflect the interwell zone. As shown in Fig. 5, there is good agreement between actual values of $k_g h$ and those calculated from Eq. 7.

These results indicate that when the ratios $\frac{r_f}{r_w}$ and $\frac{r_e}{r_f}$ are sufficiently large (discussed later) the permeability-thickness product for the fractured and unfractured zones can be estimated from the two approximately straight-line portions of the drawdown curve by using Eq. 7, although Eq. 7 originally was developed for unfractured wells. Hurst[7] has developed the corresponding analytical solution for the case of a slightly compressible flowing fluid in a system of infinite external extent. His approximation for long times confirms this conclusion in the case of the unfractured zone.

RADIUS OF FRACTURED AREA

If $\frac{r_f}{r_w}$ and $\frac{r_e}{r_f}$ are large enough (discussed later) that the analysis of Ref. 5 may be applied, an estimate for fracture radius r_f may be obtained using drawdown test results. The equation is

$$r_f = (1.5)\left[\frac{2.634 \times 10^{-4} k_1 \bar{p}t'}{\mu \phi}\right]^{\frac{1}{2}} \left[\frac{k_g}{k_1}\right]^{\frac{k_1}{2[k_1 - k_g]}} \quad . \quad . \quad . \quad . \quad . \quad . \quad . \quad . \quad . \quad . \quad . \quad . \quad . \quad (8)$$

$$\text{AT} \quad r_f, p_1 = p_2$$

$$k_1 \frac{\partial p_1}{\partial r} = k_g \frac{\partial p_2}{\partial r}$$

FIG. 4—DIAGRAM OF SYSTEM ASSUMED FOR FRACTURED WELL.

TABLE 4—PROBLEM CONDITIONS FOR SOLUTIONS 4 AND 5

All conditions of Table 1, where applicable, with the following additions and changes.

Solution	r_f (ft)
4	12
5	104

k_1 = 6 md, q_g = 2,800 Mcf/D, r_e = 1,665 ft for both solutions.

where t' is the time at which the two straight-line portions of the drawdown curve, when extrapolated, intersect. Eq. 8 is derived in the Appendix. When Eq. 8 was applied to the Solution 5 results plotted in Fig. 5, a value for r_f of 87 ft was calculated, which compares well with the actual value of 104 ft used as data for Solution 5.

MINIMUM VALUES OF r_e/r_f AND r_f/r_w

Minimum values of $\frac{r_f}{r_w}$ and $\frac{r_e}{r_f}$ with which Eqs. 7 and 8 may be applied are not known. It is probable that these values depend somewhat on k_1 and k_g. In Solution 5, where $r_e/r_f \cong 16$, $r_f/r_w \cong 200$, Eqs. 7 and 8 can be used.

STABILIZED FLOW

If r_f is known and permeability-thickness products for the fractured and unfractured zones are known, $(p_f^2 - p_L^2)$ may be calculated for stabilized conditions using the following approximation.

$$(p_f^2 - p_L^2) = \frac{1424\ \overline{\mu Z}T}{k_g h}\left[\frac{k_g}{k_1}\ln\frac{r_f}{r_w} + \ln\frac{.606 r_e}{r_f}\right]q_g \quad \ldots\ldots\ldots\ldots\ldots\ldots (9)$$

Eq. 9 is the same as Eq. 6 except that in Eq. 9 the sum of the resistances of the fractured and unfractured zones is included. Eq. 9 has been verified from other gas-problem solutions than those presented herein. Solutions 4 and 5 were not carried to times sufficiently large for stabilized flow.

TREATMENT OF FRACTURE AS A NEGATIVE SKIN

A well-known alternate method of treating fractured wells is to consider only the second straight-line portion of the drawdown curve, evaluating the skin factor S from this. When S is known, the term in brackets on the right-hand side of Eq. 9 can be replaced by $S + \ln\left(\frac{.606\ r_e}{r_w}\right)$.

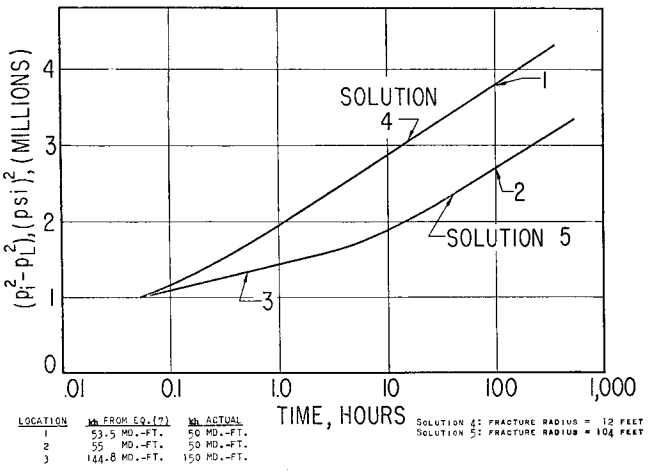

FIG. 5—CONSTANT-RATE DRAWDOWN CURVES FOR FRACTURED GAS WELLS.

TYPE 3 PROBLEMS—UNFRACTURED WELLS PRODUCED THROUGH CRITICAL FLOW PROVER

A critical flow prover is often used in testing gas wells. This device imposes a condition on the well which is neither constant rate nor constant pressure, but defines rate as a function of pressure. This function is determined by the orifice size of the critical flow prover and the pressure drop in the flow string between sand face and critical flow prover due to gravity head and friction loss. It has been assumed in the following that there were no other sources of pressure drop.

Fig. 6 shows the calculated relationship between pressure and rate imposed at the sand face as calculated for a 6,000-ft well producing through 2-in. tubing with ½ and 1½-in. diameter orifices at the surface.

Fig. 7 shows a portion of the pressure and rate history for the following system: (1) a well with properties given in Table 1; (2) a non-Darcy flow correction of Eq. 1 with a B_1 value of about 0.042, based on the correlation with porosity and permeability of Ref. 1 assuming a gas gravity gravity of 0.7; and (3) subject to the ½-in. orifice condition of Fig. 6 (Solution 6). The rate curve in Fig. 7 is nearly constant.

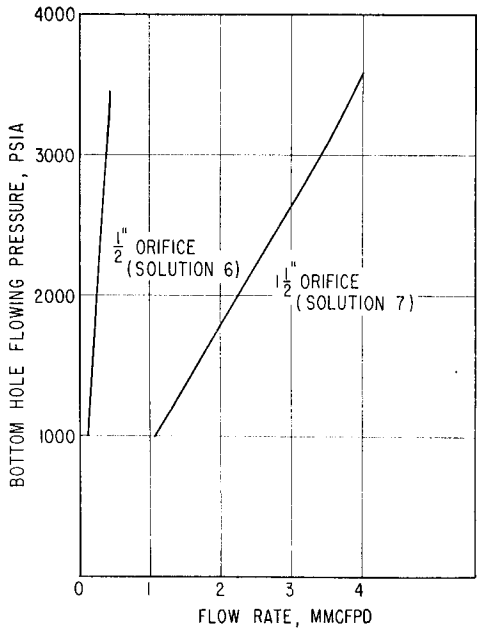

FIG. 6—CRITICAL-FLOW-PROVER BOUNDARY CONDITIONS.

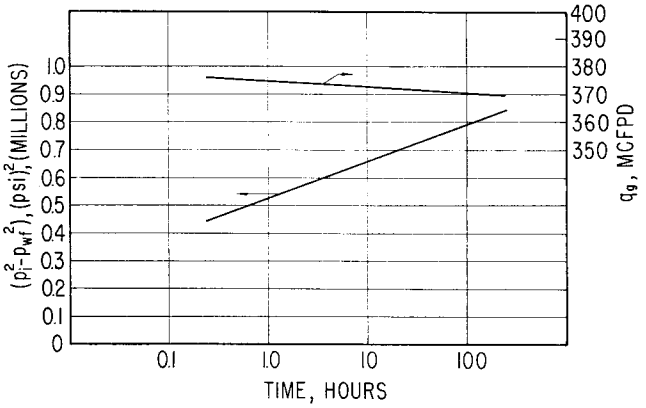

FIG. 7—GAS-WELL BEHAVIOR WITH CRITICAL FLOW PROVER (½-IN. ORIFICE, SOLUTION 6).

Fig. 8 shows a portion of the pressure and rate history for the same system except subject to the 1½-in. orifice condition of Fig. 6 (Solution 7), and also a computer-generated solution for a constant rate of 2,800 Mcf/D. This latter solution is the same as Solution 1 except for a correction for non-Darcy flow. The critical-flow-prover rate curve shown in Fig. 8 varies appreciably with time.

These results indicate that the use of a small orifice through which the well will produce at a low rate will result in a more nearly constant-rate test than the use of a larger orifice. Also, these results show that the slope of the critical-flow-prover ($p_i^2 - p_{wf}^2$) curve is lower than the slope of comparable constant-rate tests. Therefore, it is concluded that use of slopes taken from high flow-rate tests, when used with the associated flow rates and Eq. 7, will yield values for permeability-thickness product which are too high.

Also included in Fig. 8 are points calculated from the critical-flow-prover results to correct these results to the corresponding 2,800 Mcf/D constant-rate test. The equation used is

$$(p_i^2 - p_{wf}^2)_{\text{Constant Rate}} = \frac{p_{\text{Base}}}{p_{wf}}(p_i^2 - p_{wf}^2)_{\text{Critical Flow Prover}} \quad \ldots\ldots\ldots\ldots\ldots\ldots\ldots\ldots (10)$$

where p_{Base} is p_{wf} read at the time at which the flow rate is that to which the constant-rate curve is to correspond. This approximation is similar to one developed by Cornell,[6] except that the term $\frac{p_{\text{Base}}}{p_{wf}}$ is inverted in Cornell's equation. Good agreement is shown in Fig. 8 between points calculated using Eq. 10 and the computer-generated results. These results indicate that Eq. 10 may be used to correct critical-flow-prover data to constant-rate conditions.

CONCLUSIONS

1. A correlation is shown between the solutions to the problems of Type 1 presented in this paper (constant flow rate, unfractured wells) and the corresponding diffusivity-equation solution which depends on instantaneous values of $\bar{p}$, $\bar{\mu}$ and $\bar{Z}$. This correlation can be used to predict transient laminar-flow behavior for an infinite system.

2. The existence of a fracture complicates the drawdown curve. When the ratios $\frac{r_f}{r_w}$ and $\frac{r_e}{r_f}$ are large, the drawdown curve may exhibit two straight-line segments which can be used with Eq. 7 to evaluate permeability-thickness products in the fractured and unfractured zones. Using results from an analytical solution, a method has been developed which can be used for approximating fracture radius when $\frac{r_f}{r_w}$ and $\frac{r_e}{r_f}$ are large (Eq. 8). Acceptable agreement between values of permeability-thickness product and fracture radius used in the computer calculations and those calculated from Eqs. 7 and 8 using computer results were obtained for $\frac{r_e}{r_f} \cong 16$, $\frac{r_f}{r_w} \cong 200$.

3. Critical-flow-prover tests yield a drawdown curve which has a lower value for slope than do constant-rate drawdown tests at comparable rates. An approximation is given for converting critical-flow-prover test results to those which would be obtained under constant-rate conditions.

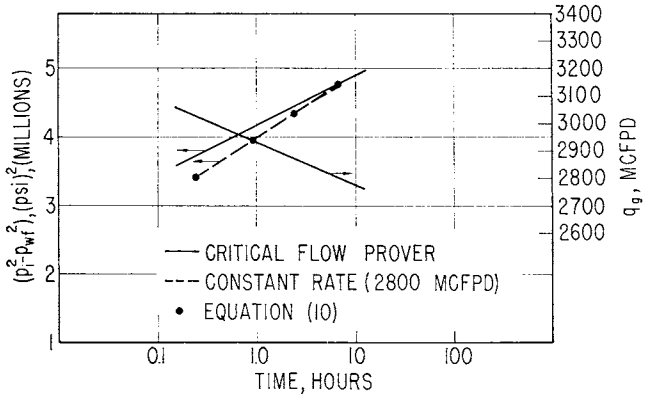

FIG. 8—GAS-WELL BEHAVIOR WITH CRITICAL-FLOW-PROVER AND CONSTANT-RATE TEST (1½-IN. ORIFICE, SOLUTION 7).

NOMENCLATURE*

R = ln r
$M(p)$ = gas mobility, defined by Eq. 3A of the Appendix
p = pressure, psia
$f(R)$ = function of R in Eq. 2 proportional to e^{2R}
h = pay thickness, ft
r = radius, ft
T = temperature
Z = gas compressibility factor
q_g = gas-production rate, Mcf/D
B_1 = non-Darcy flow coefficient, (psi/Mcf/D)^2
R_f = ln r_f
k_g = formation gas permeability, md
t = time, hours
p_L = flowing well pressure when flow is laminar, psia
p_{Base} = p_{wf} measured at the time at which flow rate is that to which critical-flow-prover data are corrected, psia
m = slope of drawdown curve, (psi)^2/cycle, subscript denoting spatial position
r_f = radius of fractured zone, ft
k_f = effective permeability to gas in the fractured zone
R_w = ln r_w
R_e = ln r_e
r_e = external radius, ft
r_w = wellbore radius, ft
p_f = pressure at r_e
n = difference-equation subscript denoting time location
Δt = time increment, hours

REFERENCES

1. Cornell, D. and Katz, D. L.: "Flow of Gases Through Consolidated Porous Media", *Ind. Eng. Chem.* (1953) **45**, 2,145.
2. van Everdingen, A. F. and Hurst, W.: "Application of the Laplace Transformation to Flow Problems in Reservoirs", *Trans.*, AIME (1949) **186**, 305.
3. Katz, D. L., *et al: Handbook of Natural Gas Engineering*, McGraw-Hill Book Co., Inc., N. Y. (1959) Chapters 10 and 11.
4. Tracy, G. W.: "Why Gas Wells Have Low Productivity", *Oil and Gas Jour.* (Aug. 6, 1956) 84.

*For definitions of other symbols, see AIME Symbols List, *Trans.*, AIME (1956) **207**, 363.

5. Hurst, W.: "Interference Between Oil Fields", *Trans.*, AIME (1960) **219**, 175.
6. Cornell, D.: "New Method Estimates Gas Well Performance", *World Oil* (Jan., 1953) 180.
7. Bruce, G. H., Peaceman, D. W., Rachford, H. H. and Rice, J. D.: "Calculations of Unsteady-State Gas Flow Through Porous Media", *Trans.*, AIME (1953) **198**, 79.

APPENDIX

METHOD USED IN NUMERICAL SOLUTION OF GAS-WELL PROBLEM

The difference equations used in the numerical solution of Eqs. 2 and 3, and equations of Fig. 5 are as follows.

INTERIOR

(In the following, equally spaced locations on the ln radius scale are denoted by integral values of m.)

$$\left\{ p_{m-1}\left[M_{m-\frac{1}{2}}\right] + p_m\left[-\left(M_{m+\frac{1}{2}} + M_{m-\frac{1}{2}} + 2F_m(1/Z_m)\right)\right] + p_{m+1}\left[M_{m+\frac{1}{2}}\right]\right\}_{n+1} = -\left\{ p_{m-1}\left[M_{m-\frac{1}{2}}\right] + p_m\left[-\left(M_{m+\frac{1}{2}} + M_{m-\frac{1}{2}} - 2F_m(1/Z_m)\right)\right] + p_{m+1}\left[M_{m+\frac{1}{2}}\right]\right\}_n \quad (1A)$$

where

$$F_m = \left(\frac{\pi \times 520}{14.7T}\right)\left(\frac{\phi h\,\Delta R}{\Delta t}\right)\left(e^{2R_{m+\frac{1}{2}}} - e^{2R_{m+\frac{1}{2}}}\right) \quad . \quad (2A)$$

and

$$M(p) = (2.703 \times 10^{-6} \times 520)\frac{khp}{T\mu Z} \quad . \quad (3A)$$

EXTERIOR

Inside Boundary (Well)

$$\frac{M_{\frac{1}{2}}}{\Delta R}(p_1 - p_o)_n = q_{gn} = \text{constant} \quad . \quad (4A)$$

(constant rate)

or

$$f[q_g]_n = \left\{[\tfrac{1}{2}(P_0 + P_1)]^2 - B_1 q_g^2\right\}_n^{\frac{1}{2}} \quad . \quad (5A)$$

(critical flow prover)

where $f(q_g)$ is determined from Fig. 6 and q_g is defined by Eq. 4A.

Outside Boundary

$$M_{m_e+\frac{1}{2}} = 0 \quad . \quad (6A)$$

where m_e is the last space point at which the solution is calculated.

An interpolation sub-routine (third difference) was used to evaluate the pressure functions μ and Z.

From the problem determined by Eqs. 1A, 4A and 6A, the solution was obtained as follows. Initial estimates for the unknown values $p_{m,n+1}$ were taken as the previously calculated values $p_{m,n}$. Then values of F_m and $M_{m-\frac{1}{2}}$ were calculated and combined as the coefficients of $p_{m,n+1}$, as indicated in the difference equations. The resulting set of linear equations was of the form to which the Thomas method[7] could be applied. This method was used to calculate values for $p_{m,n+1}$ which, in turn, were used to re-evaluate the $p_{m,n+1}$ coefficients. Solutions were considered to have been obtained when $\left|\frac{p_i - p_{j-1}}{p_j}\right| < 10^{-5}$, where j indicates the jth iteration.

Computing time on the IBM 650 was approximately 0.3 minutes per time step per space point for the constant-rate case, but much longer for the critical-flow-prover case. Work with an earlier program indicated that computing time could be considerably reduced if the initial estimates were obtained by extrapolation. However, use of the program has not warranted this change.

In the solution of the critical-flow-prover problems, Eq. 5A was replaced by

$$\tfrac{1}{2}[q_0 + q_1]_j = \tfrac{1}{2}[q_0 + q_1]_{j-1} + \omega[p_{wf_{j-1}} - f(q_{g_{j-1}})] \quad . \quad (7A)$$

where j is the jth iteration and ω is a weighting factor.

A maximum of 19 space increments were used. The validity of the solutions was checked by (1) comparing the reservoir gas content with rate integration results, and (2) repeating the early time history of the solutions using much smaller time and space increments. Only that early portion of the original solution was used which agreed within plotting accuracy with the solution obtained with reduced values of time and space increments. The time increment was increased at each step so that $t_{n+1} = ct_n$.

DERIVATION OF EQ. 8

Before the transient has reached r_f, $p_D(t_D)$ for a fractured well can be approximated for a time by $\frac{1}{2}(\ln t_D + .80907)$ if $\frac{r_f}{r_w}$ is large enough.[2] After the transient has passed the fracture, $p_D(t_D)$ can be approximated for a time by[5]

$$\frac{1}{2}\left[-\mathrm{Ei}\left(-\frac{1}{4t_D}\right) + \mathrm{Ei}\left(-\frac{r_f^2}{r_w^2\,4t_D}\right) - \frac{k_1}{k_g}\mathrm{Ei}\left(-\frac{r_f^2 k_1}{4r_w^2 k_g t_D}\right)\right]$$

if $\frac{r_e}{r_f}$ is large enough. In both cases t_D is in terms of k_1.

At the intersection of the two approximately straight-line portions,

$$\frac{1}{2}(\ln t_D + .809) = \frac{1}{2}\left[2\ln\frac{r_f}{r_w} + \frac{k_1}{k_g}\left(\ln t_D \frac{r_w^2 k_g}{r_f^2 k_1} + 0.80907\right)\right],$$

in which the Ei terms have been replaced by the logarithmic approximation valid for small values of the argument. Solving for r_f leads to Eq. 8. ★★★